Progress In Electromagnetics Research Letters, Vol. 51, 127–133, 2015

Novel Tri-Band Bandpass Filter with High Selectivity

Liangzu Cao[1, 2] and Lixia Yin[2, *]

Abstract—This paper presents a tri-band bandpass filter (BPF) consisting of a wide BPF and two narrow bandstop filters (BSFs). BPF is a ninth-order interdigital structure, and BSFs are designed fifth-order series resonators with quarter wavelength transmission line connected. The selectivity of BPF and the bandwidth of BSF are analyzed using simulation software. A tri-band BPF, made of metal cavities, is designed and measured. Three passbands are located in 1.332∼1.401 GHz, 1.443∼1.458 GHz, 1.506∼1.660 GHz, and insertion losses in passbands are less than 2.1 dB. Ratios of $\Delta f_{40\,\mathrm{dB}}/\Delta f_{3\,\mathrm{dB}}$ are 1.9, 2.67 and 1.33, respectively, and isolation between passbands is more than 75 dB. The good agreement between the simulated and measured results validated the proposed structure.

1. INTRODUCTION

Multi-band communication systems have been getting much attention. The tri-band bandpass filters with various specialities are key in the design of transmitters and receivers. Many design approaches have been published. They are divided into several categories: (1) tri-section stepped-impedance resonators (TSSIRs) [1–3], whose the centre frequencies of triple passbands depend on the impedance ratios when electric length (θ_i) of each section is equal, (2) stub loaded resonators (SLR), including single or multi-stub loaded resonators [4–7] and square ring loaded resonator (SRLR) [8], because stubs are used to control the passband and open stubs independently to produce transmission zeros, (3) transmission zeros to construct triple passbands or split a single passband to tri-band [9–11], (4) three single-band sub-filters with matching junctions [12], (5) combination of dual-mode resonator and half-wavelength resonator [13, 14], (6) multilayer substrate technique, such as LTCC [15], (7) special structures, such as Hilbert-fork resonators [16]. However, it is difficult for many structures to tune centre frequencies, and the isolation between adjacent passbands needs to be improved. In this letter, a high selectivity tri-band BPF is proposed. The filter employs one bandpass filter made of nine resonators and two bandstop filters both made of five resonators.

2. DESIGN PROCEDURE

In this paper, we propose a tri-band filter consisting of a bandpass filter and two bandstop filters, shown in Figure 1.

2.1. Circuit Design

We design a tri-band filter: 1.35∼1.40 GHz, 1.44∼1.46 GHz, 1.50∼1.65 GHz, whose attenuations are more than 50 dB at 1.2 GHz and 1.8 GHz.

Received 13 December 2014, Accepted 4 February 2015, Scheduled 4 March 2015

* Corresponding author: Lixia Yin (ty1897989@163.com).

[1] School of Electric and Optical Engineering, Nanjing University of Science & Technology, Nanjing 210014, China. [2] School of Mechanical and Electric Engineering, Jingdezhen Ceramics Institute, Jingdezhen 333001, China.

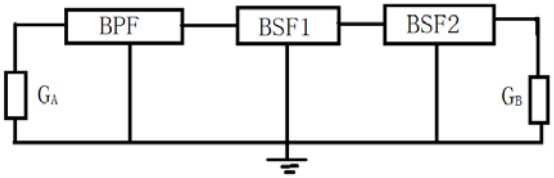

Figure 1. Diagram of tri-band filter.

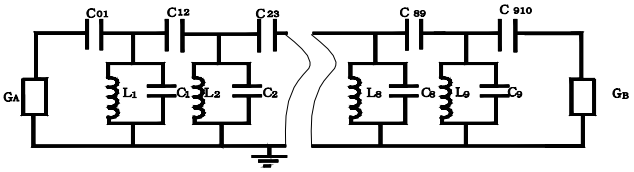

Figure 2. Equivalent circuit of nine poles bandpass filter.

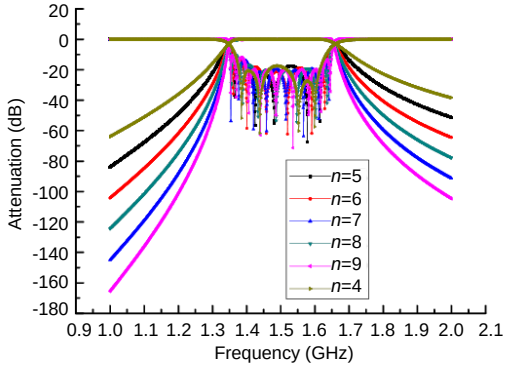

Figure 3. Responses of bandpass filters with various poles.

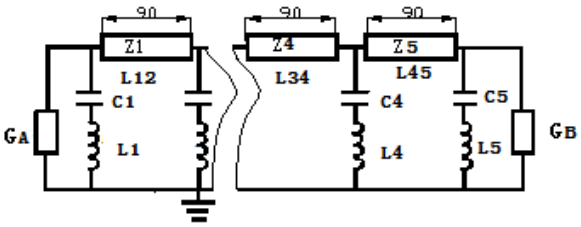

Figure 4. Equivalent circuit of bandstop filter.

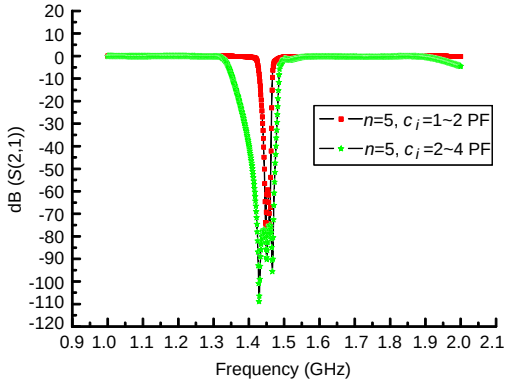

Figure 5. Response of 5th-order bandstop filter.

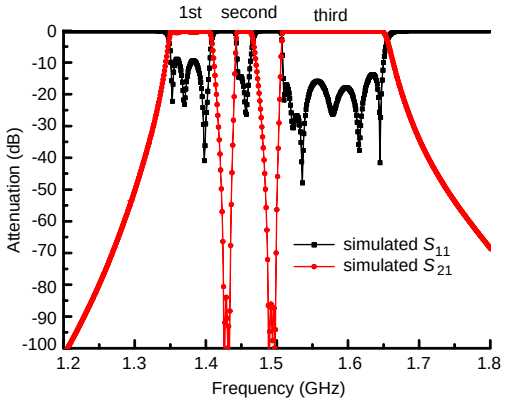

Figure 6. Simulated response of tri-band filter.

At first, a wide bandpass filter (1.35 GHz∼1.65 GHz) is designed by using Chebyshev lowpass prototype and admittance transformation. Typical bandpass filter can be equivalent to coupled cascaded resonators, shown in Figure 2.

In Figure 2, L_i and C_i ($i = 1\sim9$) form parallel resonators and can be realized by microstrip line, stripline, coaxial line and waveguide, etc. $C_{i,i+1}$ is a coupling capacitor, which denotes the coupling between adjacent resonators, and is realized by either lumped element or distributed parameter, such as parallel coupling line. The selectivity of filter is improved by either adding resonators or inserting transmission zeros. Figure 3 shows the responses of filters with various poles. The larger is the number of resonator, the sharper is the stopband. Nine resonators are selected to increase stopband attenuations in this paper.

Second, we design two narrow bandstop filters, whose center frequencies are 1.42 GHz and 1.48 GHz, respectively. Similar to bandpass filter, adding resonators can improve the selectivity of bandstop filter.

Figure 4 shows equivalent circuit of fifth-order bandstop filter. Z_i ($i = 1\sim5$) is a quarter wavelength transmission line. L_i and C_i ($i = 1\sim5$) form a series of resonators, whose resonant frequency is equal to centre frequency of bandstop filter. Note that series capacitor, C_i, affects the bandwidth of bandstop filter. Figure 5 shows the responses of bandstop filters with various capacitances. The bigger is the capacitance, the wider is the bandwidth of bandstop filter.

Last, bandpass filter and bandstop filters are directly connected together without impedance matching networks. The simulated response of tri-band filter is shown in Figure 6, which indicates that Figure 1 is feasible.

2.2. Design of Bandpass Filter Structure

The bandpass filter is designed as an interdigital filter due to larger coupling between adjacent resonators than combline filter, shown in Figure 7. The coupling coefficient (k_{ij}) between adjacent rods of interdigital filter is three times larger than that of combline filter. Figure 8 presents the structure of an interdigital filter consisting of parallel coupled lines with electrical length about $\pi/2$, in which their ends are alternately shorted-circuit and opened-circuit.

Figure 9 shows the relationship between Q_e and position of I/O feed lines. Q_e varies from 3 to 8 when t is from 11 to 23 mm, which satisfies the demand of wideband passband filter.

Ninth-order bandpass filter is designed by using Cameron Synthesis Techniques. The normalized coupling coefficients are listed as following: $M_{01} = M_{910} = 0.9145$, $M_{12} = M_{89} = 0.7615$, $M_{23} = M_{78} = 0.5700$, $M_{34} = M_{67} = 0.5383$, $M_{45} = M_{56} = 0.5300$. Based on Figure 7 and Figure 9, physical dimensions of interdigital filter are calculated and optimized by HFSS13.0. Figure 10 presents simulated response of bandpass filter.

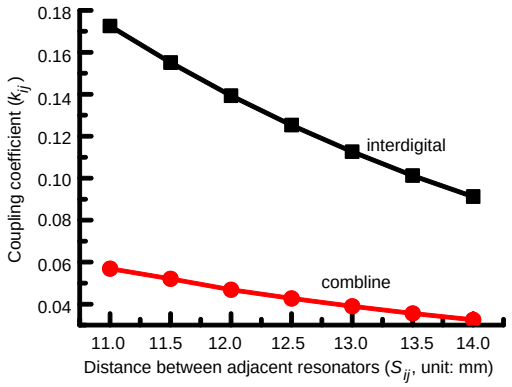

Figure 7. Coupling coefficient comparison.

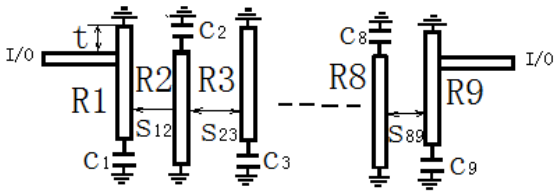

Figure 8. Stucture of nine poles bandpass filter.

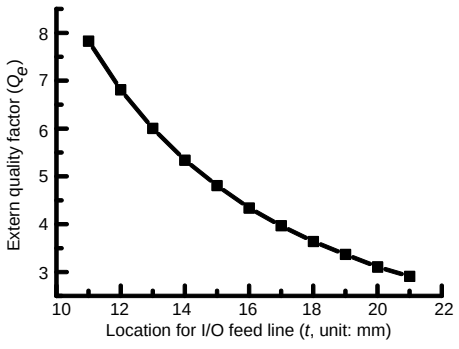

Figure 9. External quality factor (Q_e) as function of I/O feed lines.

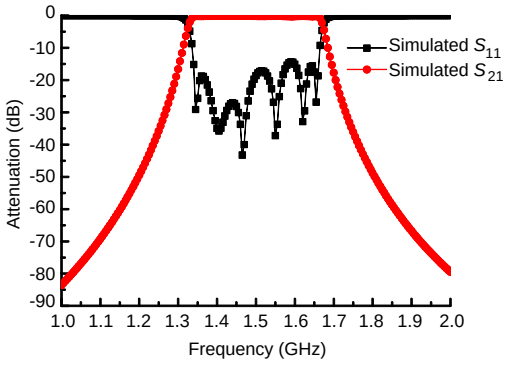

Figure 10. Simulated response of 9th-order bandpass filter.

2.3. Design of Bandstop Filter Structure

In order to improve the attenuation in stopband and lower the insertion loss in passband, series inductor L_i in Figure 4 is replaced by less than quarter wavelength coaxial resonator filled with air. The unloaded Q (Q_u) value of coaxial resonator is decided by the ratio of outer diameter (D) and inner diameter (d) and dielectric loss of dielectric material filled. Dielectric ceramic with high permittivity can reduce the size, but Q value limits its use in this filter. When D/d is 3.5, Q_u is the highest.

Series C_i is decided by

$$\omega C_i = \frac{1}{Z_i \tan\theta_i} \tag{1}$$

where θ_i and Z_i are electric length and characteristic impedance of each coaxial resonator, respectively.

The Q value of C_i also affects the performance of the filter. Conventional capacitors cannot satisfy the requirements due to capacitance fixed and Q value limited. A gap capacitor is formed between inner conductor of coaxial resonator and tuning rod connected to quarter wavelength microstrip line, shown in Figure 11.

With tuning rod unchanged, frequency of each resonator is tuned by the length of inner conductor, shown in Figure 12, and 3 dB bandwidth basically keeps constant.

The length of tuning rod is tuned based on 3 dB bandwidth of each series resonance. Figure 13 presents 3 dB bandwidth as a function of tuning rod.

$BW_{3\,\mathrm{dB}}$ is related with the capacitance of series capacitor (C_i), and the more is the capacitance, the more is $BW_{3\,\mathrm{dB}}$. Figure 12 shows the relationship between f_r and $BW_{3\,\mathrm{dB}}$ with length of tuning rod, which can be explained by Equation (1).

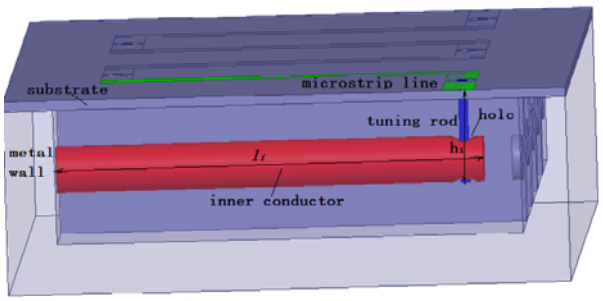

Figure 11. Structure of single resonator of bandstop filter.

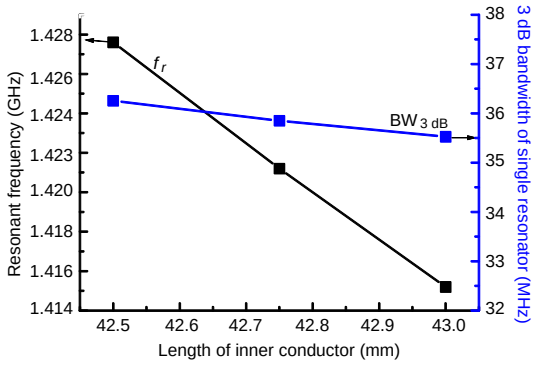

Figure 12. Resonant frequency of single resonator.

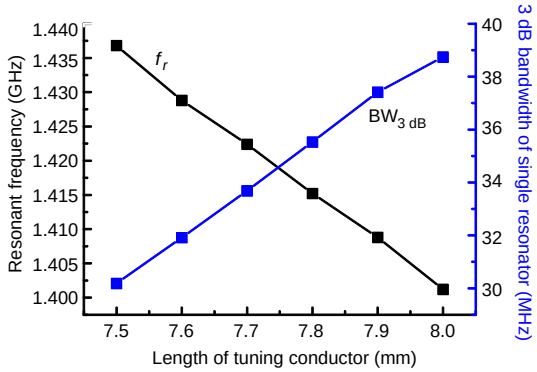

Figure 13. 3 dB bandwidth of single resonator.

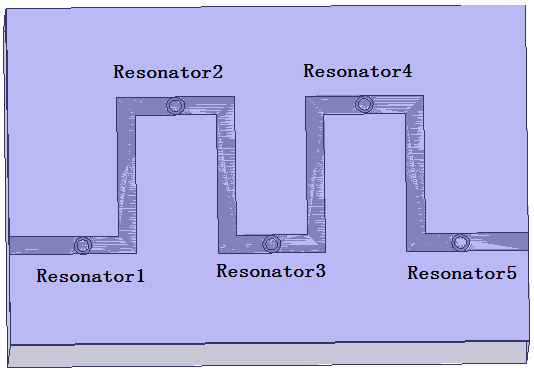

Figure 14. Structure of microstrip line connected to tuning rods.

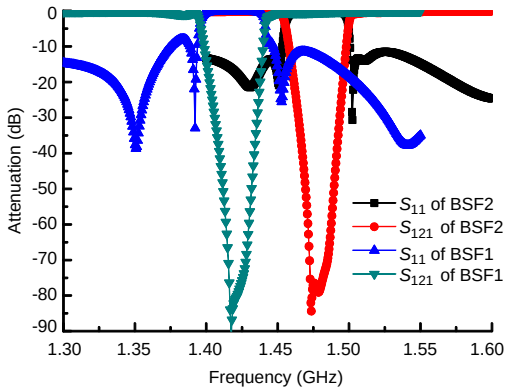

Figure 15. Simulated response of two bandstop filters connected together.

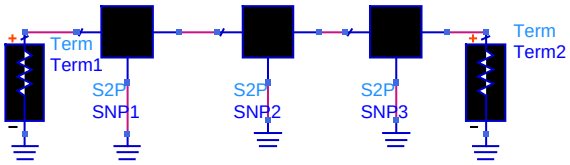

Figure 16. ADS model from data of HFSS models.

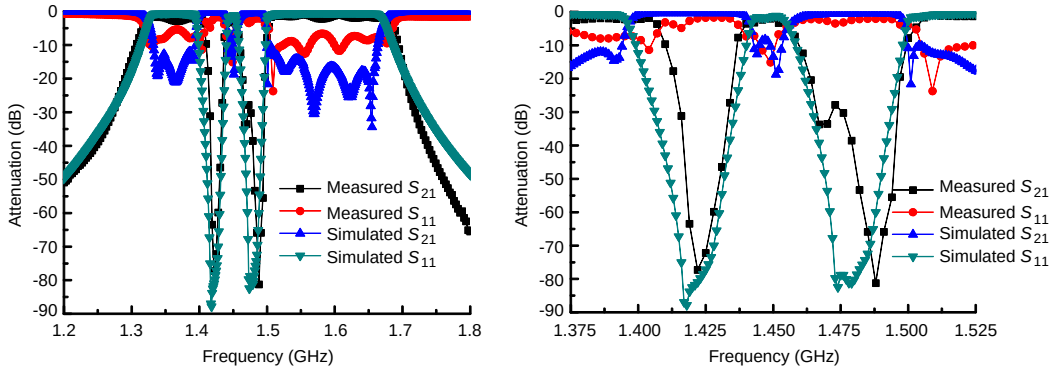

Figure 17. (a) Simulated response and measured response of tri-band filter. (b) Enlarged figure of the second passband bandpass filter.

Five inner conductors are alternately mounted on both sides of metal cavity to arrange microstrip line, shown in Figure 14.

Figure 15 presents simulated responses of fifth-order bandstop filters.

2.4. Tri-band Bandpass Filter

The solution data of HFSS model, whose file format is .s2p, are imported to 2-port component of ADS model, shown in Figure 16.

Simulated response of tri-band bandpass filter is displayed in Figure 17.

3. DESIGN EXAMPLE

The proposed filter was made of metal round rods of diameter 5 mm in a metal cavity, because of high unloaded Q value. Physical dimensions of interdigital bandpass filter are $t = 16$ mm, $s_{12} = 6.3$ mm, $s_{23} = 7.8$ mm, $s_{34} = 8.1$ mm.

Physical dimensions of the first bandstop filter are $l_1 = 43$ mm, $l_2 = 42.2$ mm, $l_3 = 41.1$ mm, $h_1 = 7.8$ mm, $h_2 = 8.0$ mm, $h_3 = 8.4$ mm, that of the other are $l_1 = 42.1$ mm, $l_2 = 40.5$ mm, $l_3 = 39.1$ mm, $h_1 = 7.4$ mm, $h_2 = 7.8$ mm, $h_3 = 8.2$ mm.

$\lambda_g/4$ transmission lines are made of microstrip on Teflon substrate which has dielectric constant of 2.2 and thickness of 1 mm.

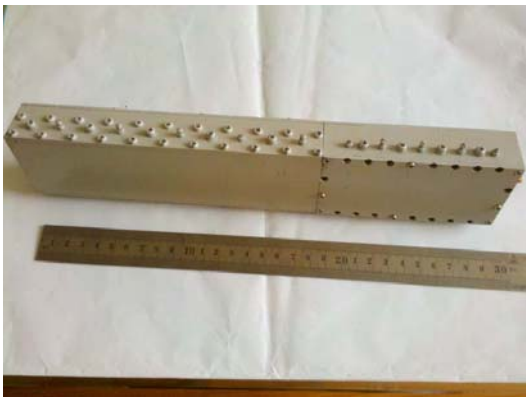

Figure 18. Photo of fabricated tri-band filter.

A bandpass filter and two bandstop filters are made of aluminium coated silver, connected together shown in Figure 1, and input and output are connected to SMA connectors and measured using Vector Networks Analyzer Agilent E570B (300 kHz∼8.5 GHz). The measured response is shown in Figure 17.

Three passbands are 1.332∼1.401 GHz, 1.443∼1.458 GHz, 1.506∼1.660 GHz. Insertion losses in passbands are 1.47 dB, 2.1 dB and 1.6 dB. Selectivities represented by $\Delta f_{40\,\mathrm{dB}}/\Delta f_{3\,\mathrm{dB}}$ are 1.9, 2.67 and 1.33, respectively. The first and third passbands are wider than the desired ones, because of fabrication and dimension errors resulting in bigger coupling coefficients. Figure 18 shows a photo of the tri-band filter.

4. CONCLUSION

A high selectivity tri-band BPF is proposed using a ninth-order BPF and two fifth-order bandstop filters. The bandwidth of second passband is decided by centre frequencies of the bandstop filters. The others are related with bandwidth of BPF. The interval among three passbands is changed by the bandwidth of bandstop filters, controlled by series capacitance.

REFERENCES

1. Wei, X.-B., P. Wang, P. Gao, et al., "Compact tri-band bandpass filter using open stub loaded tri-section $\lambda/4$ stepped impedance resonator," *IEEE Microw. Wireless Compon. Lett.*, Vol. 24, No. 8, 512–514, Aug. 2014.
2. Doan, M. T., W. Q. Che, and P. L. Nguyen, "Tri-band bandpass filter using dual-mode resonators," *The 2012 Int. Conf. on Advanced Technologies for Communications*, 1–4, 2012.
3. Chu, Q. X. and X. M. Lin, "Advanced triple-band bandpass filter using tri-section SIR," *Electron. Lett.*, Vol. 44, No. 4, 295–296, 2008.
4. Gao, L., X. Y. Zhang, B.-J. Hu, et al., "Novel multi-stub loaded resonators and their applications to various bandpass filters," *IEEE Trans. Microw. Theory & Tech.*, Vol. 62, No. 5, 1162–1172, May 2014.
5. Nguyen, T. Q., M. T. Doan, and H. C. Ta, "Tri-band bandpass filter using two short stubs and an open stub loaded resonator," *The 2013 Int. Conf. on Advanced Technologies for communications*, 1–3, 2013.
6. Chen, F. C., Q. X. Chu, and Z. H. Tu, "Tri-band bandpass filter using stub loaded resonators," *Electron. Lett.*, Vol. 44, No. 12, 747–749, Jun. 2008.
7. Xu, J., W. Wu, and C. Miao, "Compact microstrip dual-/tri-/quad-band bandpass filter using open stubs loaded shorted stepped-impedance resonator," *IEEE Trans. Microw. Theory & Tech.*, Vol. 61, No. 9, 3187–3199, Sep. 2013.

8. Luo, S., L. Zhu, and S. Sun, "Compact dual-mode triple-band bandpass filters using three pairs of degenerate modes in a ring resonator," *IEEE Trans. Microw. Theory & Tech.*, Vol. 59, No. 5, 1222–1229, May 2011.
9. Esmaeili, M. and J. Bornemann, "Substrate integrated waveguide triple-passband dual-stopband filter using six cascaded singlets," *IEEE Microw. Wireless Compon. Lett.*, Vol. 24, No. 7, 1222–1229, Jul. 2014.
10. Quendo, C., E. Rius, A. Manchec, et al., "Planar tri-band filter based on dual behavior resonator," *Proc. Eur. Microw. Conf.*, 269–272, Oct. 2005.
11. Chen, X. P., K. Wu, and Z. L. Li, "Dual-band and triple-band substrate integrated waveguide filters with Chebyshev and quasi-elliptic responses," *IEEE Trans. Microw. Theory & Tech.*, Vol. 55, No. 12, 2569–2578, Dec. 2007.
12. Heng, Y., X. Guo, B. Cao, et al., "Tri-band superconducting bandpass filter with high selectivity," *Electron. Lett.*, Vol. 49, No. 10, 658–659, May 2013.
13. Chu, Q.-X., X.-H. Wu, and F.-C. Chen, "Novel compact tri-band bandpass filter with controllable bandwidths," *IEEE Microw. Wireless Compon. Lett.*, Vol. 21, No. 12, 655–657, Dec. 2011.
14. Mo, Y., K. Song, and Y. Fan, "Miniaturized triple-band bandpass filter using coupled lines and grounded stepped impedance resonators," *IEEE Microw. Wireless Compon. Lett.*, Vol. 24, No. 5, 333–335, Dec. 2014.
15. Huang, K., T. Chiu, and H.-B. Wu, "Compact LTCC Tn-band filter design," *Proceedings of Asia-Pacific Microwave Conference*, 1–4, 2007.
16. Jankovic, N., R. Geschke, and V. C. Bengin, "Compact tri-band bandpass and bandstop filters based on Hilbert-fork resonators," *IEEE Microw. Wireless Compon. Lett.*, Vol. 23, No. 6, 282–284, Jun. 2013.